High quality epitaxial, homogeneous anatase thin films by on-site controlled hydrolysis on $LaAlO_3$ substrates and characterization

Sudu Hakuruge Dilan Priyankara Wijekoon[a], Kosuke Ono[a], Masaru Shimomura[a], Takahiko Kawaguchi[b], Naonori Sakamoto [a,b,c], Naoki Wakiya[a,b,c*]

[a] *Graduate School of Science and Technology, Shizuoka University, 3 5 1 Johoku, Chuo Ku, Hamamatsu 432 8561, Japan*

[b] *Graduate School of Integrated Science and Technology, Department of Engineering, Shizuoka University, 3 5 1, Johoku, Chuo Ku, Hamamatsu 432 8561, Japan*

[c] *Research Institute of Electronics, Shizuoka University, 3 5 1, Johoku, Chuo Ku, Hamamatsu 432 8561, Japan*

*Corresponding author's name: Naoki Wakiya, PhD

Present address: Professor, Shizuoka University, Hamamatsu, 432-8561, Japan

Email address: wakiya.naoki@shizuoka.ac.jp

High quality epitaxial, homogeneous anatase thin films by on-site controlled hydrolysis on $LaAlO_3$ substrates and characterization

The anatase form of TiO_2 is a widely studied material due to its broad range of applications. Epitaxial anatase thin films have attracted significant attention because of their enhanced electrical and optical properties. However, fabricating anatase thin films remains challenging due to their metastability and the need for highly sophisticated fabrication techniques. On-site controlled hydrolysis is a simple, cost-effective, and rapid method for producing smooth, compact thin films on various surfaces. In this study, we demonstrate a straightforward approach to fabricating highly oriented epitaxial anatase thin films on $LaAlO_3$ substrates using different solvent mixtures. The epitaxial orientation and film quality were analyzed using X-ray diffraction pole figures and rocking curves, while surface morphology was characterized by Scanning electron microscopy and atomic force microscopy. Our results indicate that thin film quality and morphology are primarily influenced by the annealing temperature rather than the choice of solvent or titanium precursor, confirming the feasibility of a scalable, low-cost epitaxial fabrication technique for anatase thin films.

Keywords: Anatase titanium dioxide, Solid state epitaxy, on-site controlled hydrolysis

High-quality epitaxial anatase thin films were fabricated via a solvent-assisted method, with annealing temperature being the key factor, while solvent variations had minimal impact on epitaxial properties or surface morphology.

Classification: 306 Thin film/ Coatings; 504 X-ray diffraction.

1. Introduction

Titanium dioxide (TiO_2) is one of the most intensively studied, stable, inert, and dielectric materials, with applications in photocatalysis solar cells (dye-sensitized solar cells, perovskite solar cells), transparent conductors, gas sensors, photodetectors, and UV-protectors, among other metal oxides [1–10]. TiO_2 naturally exists in three polymorphic forms: rutile, anatase, and brookite. Among

these, rutile is the most thermodynamically stable phase, while anatase is a metastable phase that transforms into rutile at temperatures above 700°C [11–13]. The fabrication of high-quality epitaxial thin films of anatase has garnered significant attention due to their enhanced electrical and optical properties, which result from a lower density of grain boundaries compared to polycrystalline films [14]. Various thin film deposition techniques have been employed, including pulsed laser deposition (PLD) [15], molecular beam epitaxy (MBE) [15,16], atomic layer deposition (ALD) [17,18], sol-gel spin coating [14,19], dip coating [20], hydrothermal [21], and solvothermal methods [22–24]. However, vacuum-based and hydrothermal techniques are less energy-efficient and limit large-scale film production due to their high instrumentation costs and complexity. On the other hand, as reviewed in a study by K. Ono at al. [23] the epitaxial quality of the thin films is comparatively poor in solvent based techniques. Altogether fabrication of high-quality anatase single-crystalline thin films particularly challenging. Also reports on high quality epitaxial anatase thin film fabrication by simple cost-effective rapid techniques is rare.

$LaAlO_3$ (LAO) substrates are widely used for heteroepitaxial thin film synthesis due to their favorable properties such as high-temperature stability, chemical inertness, and the ability to achieve atomically flat surfaces [15,25,26]. At high temperatures, LAO transforms into a cubic structure while in most cases, the (001) orientation of the pseudo-cubic unit cell ($a = b = c \approx 3.791$ Å, $\alpha \approx \beta \approx \gamma \approx 90°$) has been considered during fabricating (001)-oriented anatase thin films [27,28]. Its pseudo-cubic structure has a lattice constant that closely matches the horizontal lattice parameter ($a = b \sim 3.784$ Å) of tetragonal lattice anatase TiO_2 resulting in an extremely low lattice mismatch of approximately 0.16%. This near-perfect lattice match can promote coherent epitaxial growth with minimal strain and defect formation [23,29].

The on-site controlled hydrolysis is a simple, cost effective and efficient new type of concept that allows to make continuous compact thin films of TiO_2. This technique enables precise control over the composition and morphology of the films while utilizing relatively simple equipment [30]. Although the on-site controlled hydrolysis process has been studied for the deposition of polycrystalline TiO_2 films, its potential for producing epitaxial anatase films has not been realized.

In this study, we explored the fabrication of high-quality epitaxial anatase TiO_2 thin films on LAO substrates using the on-site controlled hydrolysis method with different solvent mixtures. Our results demonstrate the feasibility of producing epitaxial anatase films with excellent crystallinity and surface smoothness. Detailed, structural, morphological analyses were conducted to elucidate the quality of the films and their potential for advanced applications. This work represents a significant step toward the scalable and cost-effective fabrication of epitaxial oxide thin films for next-generation technologies.

2. Experimental

2.1. Materials and method

Titanium tetraisopropoxide (TTIP) (Fujifilm Wako Chemicals, Wako 1st Grade, 95%) and titanium tetraisobutoxide (TTBu) (Fujifilm Wako Chemicals, Wako 1st Grade, 95%) were used as titanium precursors. 1-propanol (nPr) (Fujifilm Wako Chemicals, Guaranteed Reagent, 99.5%), 1-butanol (nBu) (MP Biomedicals, Molecular Biology Reagent), were used as alcohols. 001 oriented, single side polished LAO crystals purchased from SHINKOSHA Co. LTD. (0.5 mm thick, Ra $\leqq$ 1.0 nm) were used as substrates.

Four thin films were fabricated on 8x8 mm^2, 001 oriented LAO substrate using four different solvent combinations: TTIP in nPr, TTIP in nBu, TTBu in nPr, TTBu in nBu maintaining the water bath temperature at 0°C and temperature around the spin coater at 50 °C by onsite controlled hydrolysis described in a previous study[30]. Five cycles of spin coating were repeated to obtain approximately 150 nm of final thickness. After each cycle, the films were annealed at 150 °C for 3 minutes, followed by a final annealing step at 250 °C for 5 minutes to ensure complete drying of the film. The concentration of titanium alkoxides in all solvent mixtures were fixed at 0.12 $moldm^{-3}$. Ultimately fabricated films were annealed at 700 °C and 800 °C for 10h to obtain epitaxial thin films (Figure 1).

2.2.Characterization

All films were characterized using the X'Pert Materials Research Diffractometer (MRD, Malvern PANalytical Ltd., UK) with Cu Kα radiation (λ = 1.5406 Å). The scans included 2θ/ω scans, rocking curve (ω) measurements, azimuthal scans (ϕ), and pole figure measurements. The tension voltage was set to 45 kV, and the current to 40 mA. 2θ/ω scans were performed over a range of 18° to 55°, covering the most intense XRD peaks of anatase, with 0.02° intervals and a dwell time of 0.5 seconds per step. Rocking curve (ω) scans were conducted over a 5° range, with 0.005° intervals and a dwell time of 0.5 seconds per step. For azimuthal (ϕ) scans, measurements were taken for the LAO (101) plane and the anatase (101) plane at 2θ = 33.4°, ψ = 45°, and 2θ = 25.3°, ψ = 68.3°, respectively, using a 0.1° step size and a 0.1-second dwell time per step. Pole figure measurements were performed for the LAO substrate (101) plane over a ψ range of 40°–50° at 2θ = 33.4°, and for the anatase thin film over a ψ range of 0°– 90° at 2θ = 25.3°, with a 0.5° step size and a 0.1-second dwell time per step. The morphology of the thin film was observed using a JSM-

7001F Analytical Field Emission Scanning Electron Microscope (FE-SEM) at an acceleration voltage of 15 kV and a probe current of 8 mA, after sputtering a 10 Å gold layer to enhance the specimen's conductivity. The surface morphology data over a 2500 μm^2 area was collected with a 50/1024 μm lateral resolution using a VN-8010 Simple AFM and analyzed with Gwyddion 2.67 (open-source software). Survey spectrum of X-ray Photoelectron Spectroscopy (XPS) was recorded using an AXIS-ULTRA DLD photoelectron spectrograph with 1 eV spectral resolution and three accumulations, while narrow spectra were collected with 0.1 eV spectral resolution employing an Al Kα X-ray source. The sample surface was cleaned by argon (Ar) sputtering at 3 kV for 2 minutes before the XPS measurement. Thickness of thin films were estimated by cross-sectional images taken by FE-SEM.

3. Results and discussion

The XPS survey spectra of all thin films shown in Figure 2(a) consist only of the characteristic signals of Ti and O, apart from the adventitious C 1s peak. The Figure 2(b) shows the deconvoluted high-resolution XPS spectra of the thin film made by TTIP-nBu solvent mixture, exhibiting the spin–orbit doublets of Ti 2p at approximately 458.5 eV ($2p_{3/2}$) and 464.2 eV ($2p_{1/2}$), corresponding to area percentages of 32.8% and 67.2%, respectively. The energy separation between each doublet is ~5.8 eV, which is consistent with previously reported values. These deconvoluted spectra confirm the presence of Ti in the +4 oxidation state. The Figure 2(c) represent the deconvoluted oxygen peak of the thin film made by TTIP-nBu solvent mixture, consists of two components with different peak intensities: lattice oxygen (OL) at ~529.5 eV and hydroxides (OH) at ~531.2 eV, characteristic of TiO_2. [22,23,31]. The C 1s spectrum (Figure 2(d)) can be deconvoluted into three peaks: C-CH (284.6 eV), C-O (285.9 eV), and O=C (288.3 eV). The C-CH and C-O peaks are attributed to adventitious carbon, likely from environmental contamination. The peak at 288.3 eV

provides indirect evidence of the presence of Ti-substituted carbon in the film [32]. However, at high annealing temperatures, the likelihood of carbon atoms remaining in the thin film is very low confirming that carbon impurities in the crystal are not significant [33,34]. Overall, XPS that all the thin films are composed of Ti^{+4} state and O^{-2} state as well as are of high purity. Additionally, the absence of characteristic signals from substrate elements serves as an indirect indication that the thin films are continuous without cracks [31]. Moreover, the nearly identical high-resolution XPS spectra suggest that the surface chemical properties of all thin films are almost identical (Figure S1).

The XRD analysis of all TiO_2 thin films on LAO substrates was conducted using pole figures, omega scans, and 2θ/ω scans to evaluate crystallographic orientation, texture quality, and structural properties. The 2θ/ω scan in Figure 3 shows only the characteristic peaks of $LaAlO_3$ (001), (002), and anatase (004), confirming that all fabricated TiO_2 thin films are in the anatase phase, with $LaAlO_3$ (001) || anatase (001). A shift in peak positions of anatase (004) was observed from the stress-free position at 36.801° to 37.79° at 700 °C and to 37.72° at 800 °C. Using Bragg's law and the relationship between lattice spacing, this shift corresponds to an increase in the lattice parameters over c direction from 9.512 Å (stress-free) to 9.515 Å (at 700 °C) and 9.532 Å (at 800 °C) and the. The calculated theoretical in-plane strain is 0.20%, which, according to Poisson's relationship, indicates an out-of-plane expansion corresponding to in-plane compressive strain [19,27,28,35].

Figure 4 compares the (004) anatase peaks of thin films obtained at 700 °C and 800 °C using omega scan 2θ at 37.72° and 37.79°, respectively. As clearly seen, the Full Width at Half Maximum (FWHM) improves at 800 °C, indicating an enhancement in crystal quality compared to films annealed at 700 °C. Furthermore, the narrow peaks observed at 800 °C, with FWHM

values below 0.48° for all thin films, suggest excellent crystallinity, minimal mosaicity in the epitaxial layer, and strong substrate-film interaction during growth. However, the FWHM values for thin films fabricated using different solvent mixtures exhibit notable deviations. The minimum FWHM observed is 0.37° for the TTBu-nBu-based solvent mixture, while the maximum FWHM is 0.48° for the TTBu-nPr solvent mixture (Table 1). This variation follows a parallel trend with the FWHM of the substrate (002) peaks (Figure S3), which can be attributed to the anisotropic dependency of FWHM rocking curves due to the pseudo cubic nature of the substrate [36]. Moreover, the mean FWHM of the rocking curve is the best-reported value obtained via solvent-assisted synthesis, as confirmed by a recent research review [23].

As shown in Figure 5, the {101} planes of anatase (101, 011, -101, 0-11) are approximately 90° apart and align with the corresponding reflections of the $LaAlO_3$ substrate (101, 011, -101, 0-11). This indicates that the anatase film is not only oriented in-plane but also oriented out-of-plane on the $LaAlO_3$ substrate, following the epitaxial relationship $LaAlO_3$ [001] || anatase [001], consistent with previous reports. However, as seen in the magnified image, a 0.2° misalignment is observed, which can be attributed to strain in the film. Furthermore, no additional peaks beyond the {101} reflections or evidence of twinning were detected, further confirming the high-quality crystal orientation. The average FWHM of the ϕ scan is 0.35° where substrate is 0.18° the representing a considerable improvement in in-plane alignment compared to previously reported solvent-based synthesis methods [19,37].

The pole figures (Figure 6) for anatase (101) reflections further confirm the epitaxial relationship between the anatase film and the $LaAlO_3$ substrate, as the intensity maxima of the anatase {101} planes well align with those of the substrate. The absence of additional intensity regions suggests the absence of secondary phases or random orientations. Furthermore, the similar

characteristics of the pole figures for each film are in good agreement with other types XRD of analyses, providing evidence of identical thin film formation (Figure S2).

As previously reported by our group, smooth, compact, and continuous thin films can be fabricated on surfaces through on-site controlled hydrolysis, achieved via the partial hydrolysis of titanium alkoxides [30]. Upon low-temperature heating, these thin films convert into amorphous TiO_2, while completing hydrolysis and removing residual alcohols from the film. During high-temperature annealing, the amorphous thin films transform into highly oriented, dense epitaxial thin films through a well-studied solid-state epitaxy (SSE) process [38,39].

Figures 7 and 8 compare the surface morphology of each thin film, the substrate, and the film annealed at 250°C. As clearly observed in the SEM and AFM 3D images, all epitaxial film surfaces exhibit a similar morphology, consisting of apparently identical grains. In contrast, the SEM images show that the films annealed at 250°C have a flat, smooth surface similar to that of the substrate. It is evident that surface roughness due to grain formation emerges after annealing. This grain structure can be attributed to film shrinkage caused by the pyrolysis of residual organic materials, material rearrangement during densification, and the natural surface roughening that occurs during solid-state epitaxy [35]. Notably, fractures and bulging due to thermal stress were not observed, emphasizing that the film is continuous and firmly attached to the substrate. Furthermore, the cross-sectional SEM image (Figure 7(g)) confirms the continuity and thickness of the anatase film and the firm bond between thin film and substrate. Also, the minimal variation of surface roughness values of each thin film further confirms, the overall morphologies remain consistent across all samples, without significant differences.

All the observations align with the typical behavior of SSE, wherein an initially amorphous thin film transforms into a crystalline, epitaxially aligned structure upon thermal treatment. This

process explains the disappearance of secondary crystal phases, the enhancement of preferred orientation, shifting the peak positions and the temperature-dependent increase in XRD peak intensity. These behaviors result from a complex interplay of factors, including lattice mismatch, differences in thermal expansion coefficients (LAO thermal expansion coefficient: 12.6×10^{-6} °C^{-1}, anatase in-plane thermal expansion coefficient: 4.47×10^{-6} °C^{-1} [40,41]), thermally induced atomic mobility and rearrangement, and defect formation. Due to the complexity of these interactions, isolating the individual contribution of each factor is challenging.

From a thermodynamic perspective, single crystalline structures are more stable than amorphous ones. At elevated temperatures, atoms acquire sufficient energy to overcome the activation barrier and rearrange from a disordered to an ordered crystalline state. This leads to enhanced atomic alignment with the substrate lattice—i.e., epitaxial growth—and results in increased film density. During SSE, this crystallization typically initiates at the film–substrate interface and propagates toward the film surface. The first few unit cell layers become well-aligned with the substrate, generating significant strain. However, as the crystallization progresses, this strain is gradually relaxed. Since anatase has larger in-plane lattice parameters than both LAO and STO substrates, strain relaxation introduces increased spacing in the upper unit cells [39,42–44].

Additionally, higher temperatures increase atomic vibrations and thermal expansion in both the film and substrate, further contributing to expansion and potential misalignment in the upper layers. Consequently, the likelihood of defect formation—such as interstitials or propagating dislocations—also increases with temperature. Upon cooling to room temperature, the film and substrate contract at different rates due to their distinct thermal expansion coefficients. This differential contraction, combined with pre-existing high-temperature defects, results in in-plane compressive stress as the lattice attempts to contract. This residual strain can influence both the

position and sharpness of XRD peaks, ultimately impacting the measured crystallinity and structural quality of the film. On the other hand, at high temperatures, surface roughness may increase due to pyrolysis, density increase, and stress relaxation [39,43,44].

Two main solvent-based approaches, distinguished by their growth mechanisms, can be identified for fabricating epitaxial anatase thin films: sol-gel synthesis via solid-state epitaxy (SSE) and solvothermal/hydrothermal synthesis via liquid-phase epitaxy. In both methods, titanium alkoxides are commonly used as the precursor due to their high reactivity. To control the hydrolysis and condensation reactions, additives such as acids, ligands or chelating agents, polymers, and other solvents are typically introduced [19,20,22,23]. These result in complex mixtures that are generally colloidal solutions consisting of partially hydrolyzed species.

In sol-gel-based synthesis, the colloidal solution is spread over the substrate, forming a relatively less compact and often amorphous thin film. During annealing, this film transforms into an epitaxial layer. However, due to its initial low density, the resulting surface may be less smooth, and there is greater freedom for crystal orientation to deviate. Moreover, the non-uniformity of the film can lead to weaker regions, making it more susceptible to cracking. In contrast, solvothermal/hydrothermal synthesis can introduce impurities into the crystal lattice due to trapped additives from the solvent system. For example, fluorine was found incorporated into the lattice in a solvothermally grown film, as reported by Ono et al [23]. In both approaches, the presence of these additives can compromise the chemical purity and structural quality of the final film.

However, the on-site controlled hydrolysis method offers distinct advantages. This technique enables better control over unwanted impurities, as the reaction is regulated directly at the substrate surface. It also produces a compact amorphous film that minimizes orientation freedom during the epitaxial conversion process. Due to the uniformity and compactness of this

film, there are fewer weak regions, significantly reducing the risk of cracking. These factors contribute to the formation of high-quality epitaxial anatase films using this method.

For this study, a simple setup similar to that described in the previous work and a standard furnace were used to synthesize high-quality single crystalline thin films. As a result, the initial equipment cost is minimal compared to advanced fabrication techniques, and the scalability of the process is high. Unlike vacuum-based methods, which consume significant energy to maintain vacuum conditions and heat large assemblies, this approach requires energy primarily to heat only the substrate and thin films. The coating process is rapid, and the annealing can be performed in batches, making the overall method both energy-efficient and timesaving. Furthermore, in contrast to hydrothermal and solvothermal syntheses, this technique uses only a small amount of chemicals, resulting in minimal chemical waste. Therefore, this method simplifies the process of synthesizing high-quality epitaxial anatase films, which has traditionally been challenging to achieve. Such high-quality single-crystalline films offer enhanced charge transport due to reduced recombination losses and fewer trapping sites. As a result, these thin films can significantly improve the efficiency of photovoltaic devices, as well as the sensitivity and responsivity of the sensors. Moreover, the low defect density enhances their optical transparency and electrical conductivity, which are crucial for applications in transparent electronics and optical computing, where precise control over light propagation and minimal scattering are essential. Additionally, the (001) orientation of anatase significantly boosts photocatalytic efficiency, making these films highly suitable for environmental remediation and water splitting applications.

Additionally, the on-site controlled hydrolysis method involves several adjustable parameters such as evaporation temperature, precursor concentration, number of coatings and spin-coating rate that influence the thickness of the resulting amorphous compact film. By carefully

tuning these parameters, the thickness of the initial amorphous film can be precisely controlled[30]. Since this amorphous film is later converted into an epitaxial film through solid-state epitaxy, the final thickness of the epitaxial film is largely determined by the initial thickness of the amorphous layer, making the epitaxial film thickness controllable with similar precision. However, surface roughening during the epitaxial transformation can introduce slight variations in thickness, which should be taken into consideration in applications where precise film thickness is critical.

On the other hand, this fabrication method requires high-temperature annealing, which is a disadvantage that may limit its applicability in certain areas. Moreover, factors such as the effect of annealing temperature, film thickness, and dopability still require further investigation.

4. Conclusions

In this study, the fabrication of highly oriented epitaxial anatase thin films was successfully achieved through on-site controlled hydrolysis. As previously reported, the epitaxial relationship between the anatase film and the $LaAlO_3$ (LAO) substrate follows $LaAlO_3$ [001] || anatase [001] for all thin films synthesized using different solvent mixtures. The epitaxial quality and surface morphology of the thin films do not exhibit significant changes with variations in the solvent mixture but are primarily influenced by the annealing temperature. Therefore, the effect of the solvent or Ti precursor on epitaxial quality or morphology is negligible. Overall, this method offers a fast, simple, low-cost, environmentally friendly, and efficient approach to fabricating high quality 001 oriented anatase epitaxial thin films. Therefore, this method could accelerate the development of next-generation energy, sensing, and electronic devices with improved performance, stability, and environmental sustainability.

Acknowledgement

All the staff members of Instrumental Analysis Center, Hamamatsu campus, Shizuoka University. Part of this work was conducted under the Cooperative Research Project Program of Research Institute of Electronics, Shizuoka University. Part of this research was also supported by the Collaborative Research Project of Laboratory for Materials and Structures, Institute of Innovative Research, Institute of Science Tokyo.

Funding

Part of this work was supported by a Grant-in-Aid for Scientific Research from the Ministry of Education, Culture, Sports, Science and Technology (No. 22H01770).

Disclosure statement

No potential conflict of interest was reported by the authors.

Data Availability Statement

The data that support the findings of this study are available from the corresponding author, Naoki Wakiya, upon reasonable request.

References.

[1] Luttrell T, Halpegamage S, Tao J, et al. Why is anatase a better photocatalyst than rutile? - Model studies on epitaxial TiO_2 films. Sci Rep. 2014;4:4043.

[2] Li Y, Xia B, Jiang B. Thermal-induced durable superhydrophilicity of TiO_2 films with ultra-smooth surfaces. J Solgel Sci Technol. 2018;87(1):50–58.

[3] Soussi A, Ait Hssi A, Boujnah M, et al. Electronic and Optical Properties of TiO_2 Thin Films: Combined Experimental and Theoretical Study. J Electron Mater. 2021;50(8):4497–4510.

[4] Sathish, M., Radhika, N. & Saleh, B. Current Status, Challenges, and Future Prospects of Thin Film Coating Techniques and Coating Structures. J Bio Tribo Corros. 2023; **9:**35.

[5] Qin J, Zhang Z, Shi W, et al. The optimum titanium precursor of fabricating TiO_2 compact layer for perovskite solar cells. Nanoscale Res Lett. 2017;12:640.

[6] Nakata K, Fujishima A. TiO_2 photocatalysis: Design and applications. Journal of Photochemistry and Photobiology C: Photochem. Rev. 2012;13(3):169–89.

[7] Rzaij JM, Rzaij JM, Abass AM. Review on: TiO_2 Thin Film as a Metal Oxide Gas Sensor. J. Chem. Rev. 2020;2(2):114–21.

[8] Arconada N, Durán A, Suárez S, et al. Synthesis and photocatalytic properties of dense and porous TiO_2-anatase thin films prepared by sol–gel. Appl Catal B. 2009;86(1–2):1–7.

[9] Yamada N, Hitosugi T, Kasai J, et al. Transparent conducting Nb-doped anatase TiO_2 (TNO) thin films sputtered from various oxide targets. Thin Solid Films. 2010;518(11):3101–3104.

[10] Sato Y, Akizuki H, Kamiyama T, et al. Transparent conductive Nb-doped TiO_2 films deposited by direct-current magnetron sputtering using a TiO_2−x target. Thin Solid Films. 2008;516(17):5758–5762.

[11] Sabyrov K, Burrows ND, Penn RL. Size-dependent anatase to rutile phase transformation and particle growth. Chem. Mater. 2013:25(8):1408-1415.

[12] Hanaor DAH, Sorrell CC. Review of the anatase to rutile phase transformation. J. Mater. Sci. 2010;46(4):855–874.

[13] Tompsett GA, Bowmaker GA, Cooney RP, et-el. The Raman Spectrum of Brookite, TiO_2 (Pbca,2=8). J. Raman Spectrosc. 1995;26(1):57-62.

[14] Jung HS, Lee JK, Lee J, et al. Mobility enhanced photoactivity in sol-gel grown epitaxial anatase TiO_2 films. Langmuir. 2008;24(6):2695–2698.

[15] Krupski K, Sanchez AM, Krupski A, et al. Optimisation of anatase TiO_2 thin film growth on $LaAlO_3$(001) using pulsed laser deposition. Appl Surf Sci. 2016;388:684–90.

[16] Wang YH, Rahman KH, Wu CC, at al. A review on the pathways of the improved structural characteristics and photocatalytic performance of titanium dioxide (TiO_2) thin films fabricated by the magnetron-sputtering technique. Catalysts. 2020;10(6):598.

[17] McDaniel MD, Posadas A, Wang T, et al. Growth and characterization of epitaxial anatase TiO_2 (001) on $SrTiO_2$-buffered Si(001) using atomic layer deposition. Thin Solid Films. 2012;520(21):6525–6530.

[18] Barlaz DE, Seebauer EG. Solid phase epitaxial regrowth of (001) anatase titanium dioxide. J. Vac. Sci. Technol. A. 2016; 34(2):20603.

[19] Jung HS, Lee JK, Lee J, et al. Strain relaxation in sol-gel grown epitaxial anatase thin films. J. Phys. Chem. C. 2008;112(11):4205–4208.

[20] Oropeza FE, Zhang KHL, Regoutz A, et al. Growth of epitaxial anatase nano islands on $SrTiO_3$ (001) by dip coating. Cryst. Growth Des. 2013;13(4):1438–1444

[21] Zhang Z. A low-temperature and low-cost method to produce high-quality epitaxial anatase TiO_2 thin films. J. Mater. Res. 2005;20(2):292–294.

[22] Ono K, Shimomura M. Solvothermal Epitaxy of an Anatase TiO_2 Thin Film on $SrTiO_2$ (001) and the Effect of Precursor Composition on Its Growth. Cryst Growth Des. 2024;24(4):1798–1805.

[23] Ono K, Kimura K, Kato T, et al. Epitaxial growth of a homogeneous anatase TiO_2 thin film on $LaAlO_3$ (001) using a solvothermal method with anticorrosive ligands. Chem. Eng. J. 2023;451(3):138893.

[24] Xu H, Feng X, Luan C, et al. Preparation and characterization of single crystalline anatase TiO_2 epitaxial films on $LaAlO_3$(001) substrates by metal organic chemical vapor deposition. Scr Mater. 2016;124:76–80.

[25] Hong D, Liu C, Pearson J, et el. Epitaxial growth of high quality $SrFeO_3$ films on (001) oriented $(LaAlO_3)_{0.3}(Sr_2TaAlO_6)_{0.7}$. Appl Phys Lett. 2017; 111(23):232408.

[26] Wang WL, Peng CY, Ho YT, et al. Microstructure of a-plane ZnO grown on $LaAlO_3$ (001). Thin Solid Films. 2010 Mar 31;518(11):2967–2970.

[27] Hayward SA, Morrison FD, Redfern SAT, et al. Transformation processes in $LaAlO_3$: Neutron diffraction, dielectric, thermal, optical, and Raman studies. Phys. Rev. B. 2005;72(5): 054110.

[28] Zhao J, Angel RJ, Ross NL. The structural variation of rhombohedral $LaAlO_3$ perovskite under non-hydrostatic stress fields in a diamond-anvil cell. J. Phys.: Condens. Matter. 2011;23(17):175901.

[29] Kennedy RJ, Stampe PA. The influence of lattice mismatch and film thickness on the growth of TiO_2 on $LaAlO_3$ and $SrTiO_3$ substrates. J Cryst Growth. 2003;252(1–3):333–342.

[30] Wijekoon S.H.D.P, Shimomura M, Kawaguchi T, et al. Smooth TiO_2 thin film fabrication by on-site controlled hydrolysis of alcohol-titanium alkoxide mixtures. Surf. Interfaces. 2025;58: 105755.

[31] Granada-Ramirez DA, Cardona-Bedoya JA, Hernandez-Rojas U, et al. Assessment of Cr doping on TiO_2 thin films deposited by a wet chemical method. Ceram Int. 2023;49(18):30347–30354.

[32] Hua L, Yin Z, Cao S. Recent Advances in Synthesis and Applications of Carbon-Doped TiO_2 Nanomaterials. Catalysts. 2020;10(12):1431.

[33] Qi D, Xing M, Zhang J. Hydrophobic carbon-doped TiO_2/MCF-F composite as a high performance photocatalyst. J. Phys. Chem. C. 2025;118(14):7329–7336.

[34] Wu Y, Zhang J, Xiao L, et al. Properties of carbon and iron modified TiO_2 photocatalyst synthesized at low temperature and photodegradation of acid orange 7 under visible light. Appl Surf Sci. 2010;256(13):4260–4268.

[35] Playford HY. Variations in the local structure of nano-sized anatase TiO_2. J. Solid State Chem. 2020; 288:121414.

[36] Izumisawa F, Ishii Y, Kimura M, et al. Symmetry change in $LaNiO_3$ films caused by epitaxial strain from $LaAlO_3$, $SrTiO_3$, and $DyScO_3$ pseudocubic (001) surfaces. J. Appl. Phys. 2024;136(7):75303.

[37] Jung HS, Lee JK, Lee J, et al. Mobility enhanced photoactivity in sol-gel grown epitaxial anatase TiO_2 films. Langmuir. 2008 Mar 18;24(6):2695–2698.

[38] Ohring M. The Material science of thin films. San Diego: Academic Pres; 1992. Chapter 7, Epitaxy; p.307-353 .

[39] Olson GL, Roth JA. Kinetics of solid phase crystallization in amorphous silicon. Mater. Sci. Rep. 1988 May 3: 1-78

[40] Lanthanum Aluminate - SHINKOSHA Crystals for a bright future. Shizuoka. [Internet]. [cited 2025 May 3]. Available from: https://www.shinkosha.com/english/product/epi_substrate/lao/

[41] Hummer DR, Heaney PJ, Post JE. Thermal expansion of anatase and rutile between 300 and 575 K using synchrotron powder X-ray diffraction. Powder Diffr. 2007 Dec;22(4):352–7.

[42] Patel AR, Rao K V, Shivakumar GK. Role of Deposition Conditions, Impurities and Structural Defects in the Epitaxial Growth of Thin Films. Appl Phys. 1981; 24:85–8.

[43] Mieghem P Van, Jain SC, Nijs J, et al. Stress relaxation in laterally small, strained semiconductor epilayers. J. Appl. Phys. 1994 Jan; 75 (1): 666-668

[44] Dunstan DU. Review Strain and strain relaxation in semiconductors. J. Mater. Sci.: Mater. Electron. 1997;8:337–375.

Tables and captions

Table 1 Summary of surface properties and crystalline quality of epitaxial films

Solvent composition	FWHM of rocking curves at 700/ (degrees)	FWHM of rocking curves at 800/ (degrees)	Surface roughness (R_z) At 800/ (nm)
TTIP-nPr	0.80	0.43	15.6
TTIP-nBu	0.86	0.46	16.3
TTBu-nPr	0.75	0.48	17.6
TTBu-nBu	0.78	0.37	13.5

Figures and captions

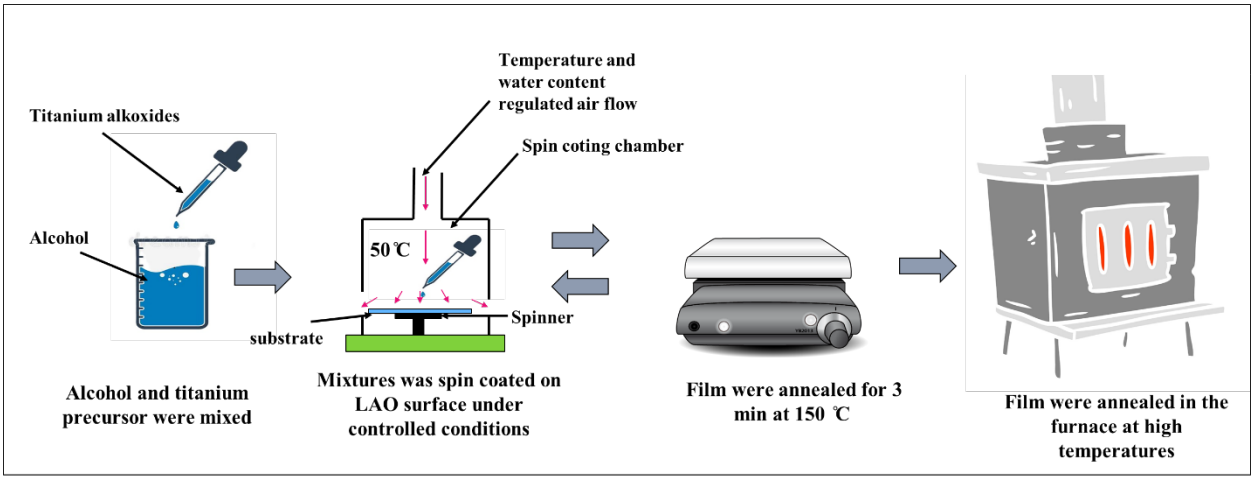

Figure 1. The schematic diagram of the procedure of synthesizing epitaxial anatase films

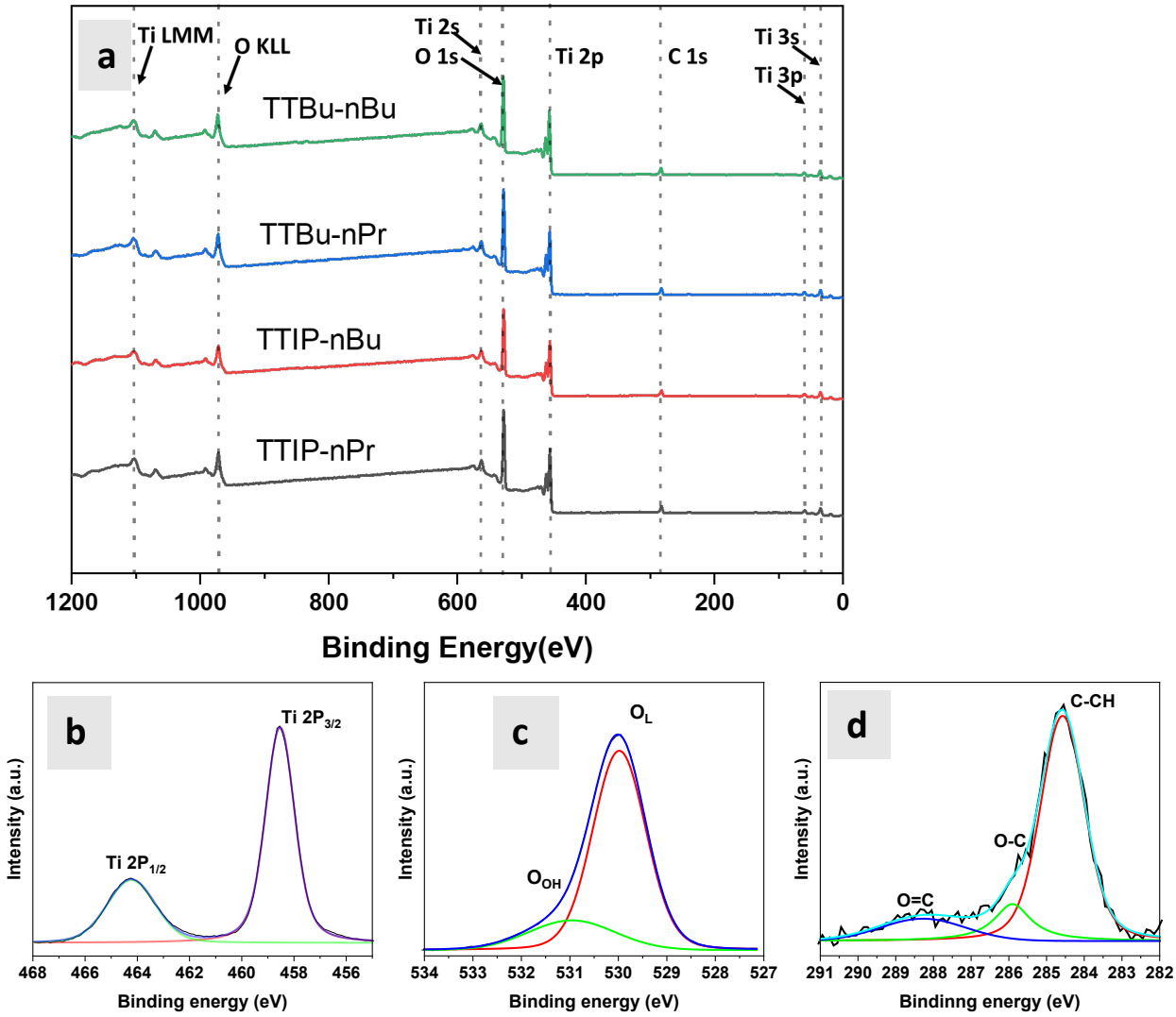

Figure 2. XPS spectra of thin films annealed at 800 °C. (a) Survey spectra obtained for different thin films made using different solvent mixtures (b) Ti 2p region of deconvoluted high resolution XPS spectrum of the film made from TTIP-nPr (c) O 1s region of deconvoluted high resolution XPS spectrum of the film made from TTIP-nPr . (d) C 1s region of deconvoluted high resolution XPS spectrum of the film made from TTIP-nPr .

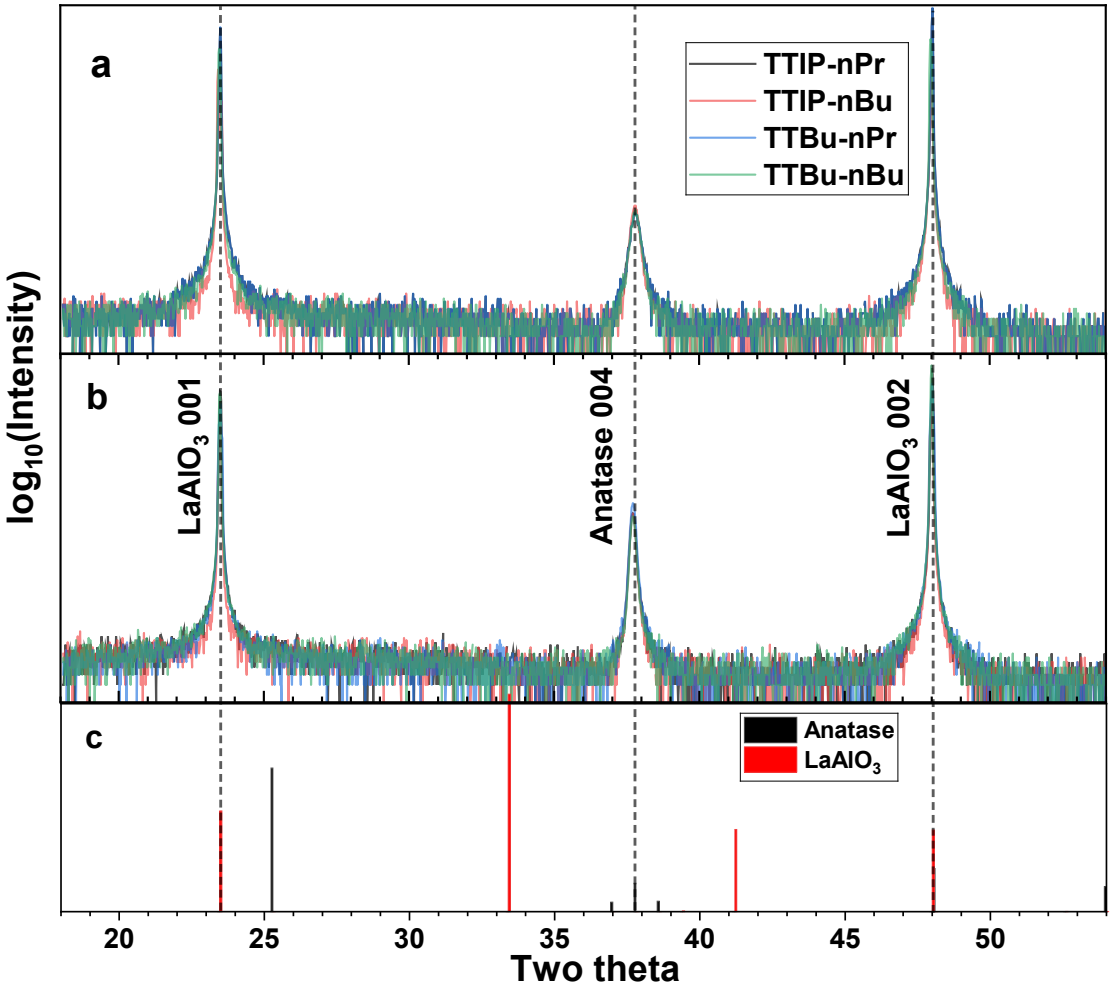

Figure 3. XRD 2θ/ω of thingies made by different solvent mixtures annealed at (a) 700 °C and (b) 800 °C **(c) reference 2θ positions of anatase and $LaAlO_3$

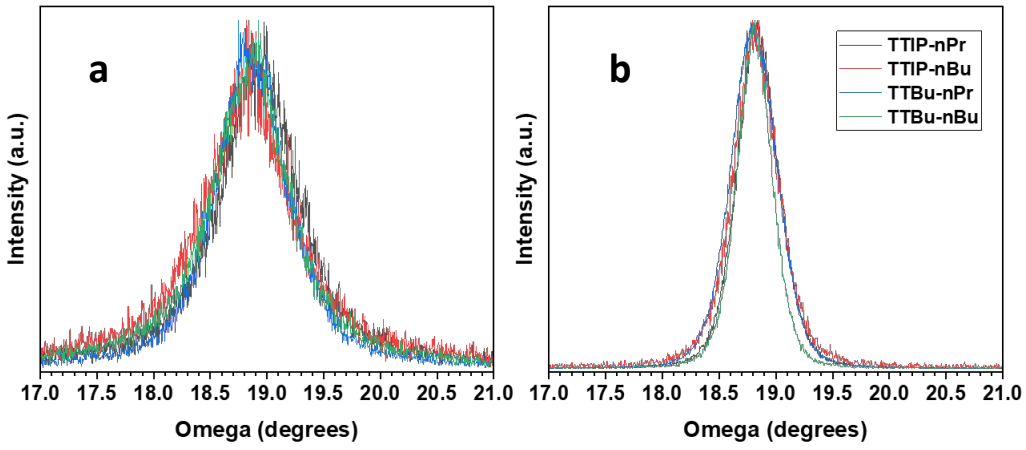

Figure 4. XRD rocking curves of the thin film made by different solvent mixtures annealed at (a) 700 °C and (b) 800 °C

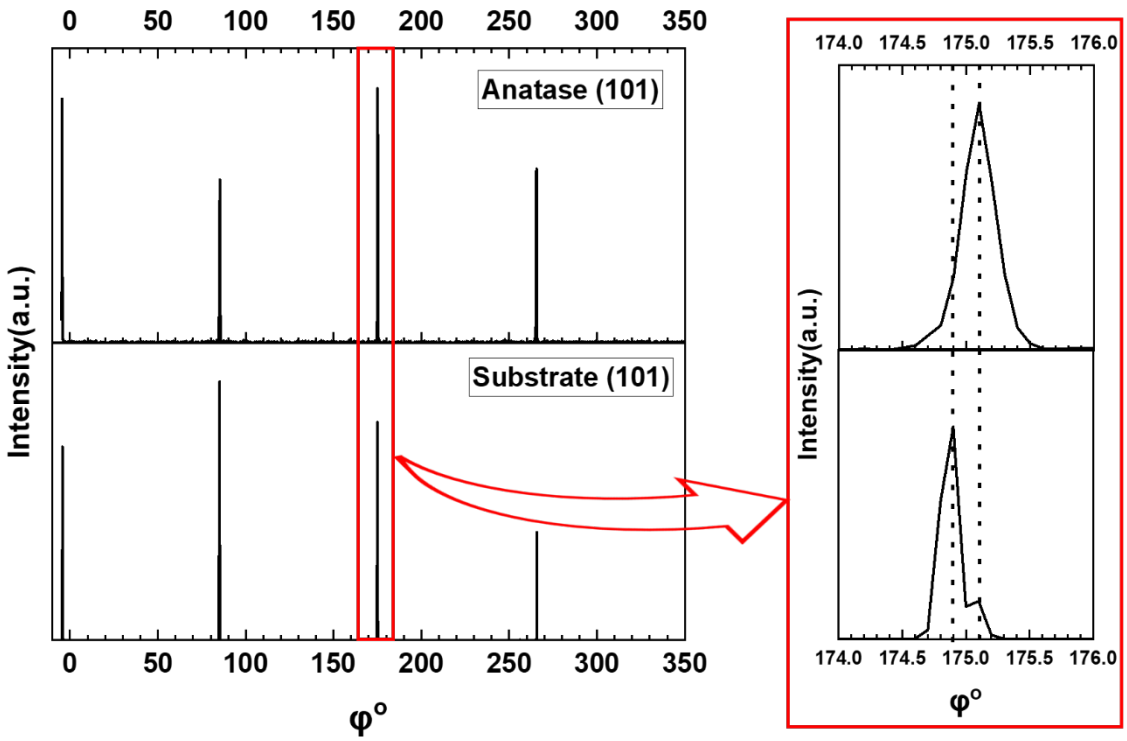

Figure 5 . XRD ϕ scan results for (101) TiO_2 and (101) at 2Θ =33.4, ψ = 45 for substrate and 2Θ = 25.3, ψ = 68.3 for anatase thin film made by TTBu-nBu solvent mixture and annealed at 800°C

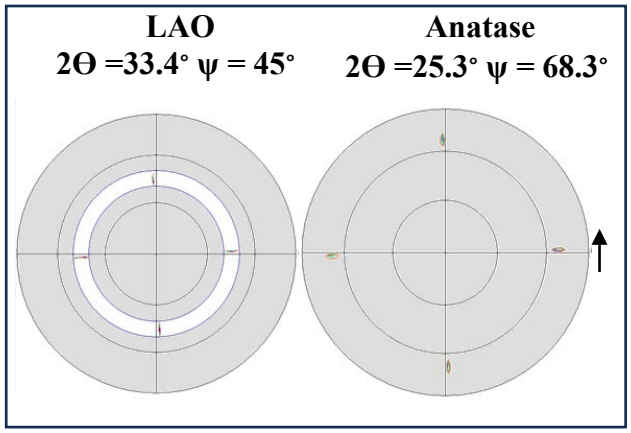

Figure 6. Orientation analysis by pole figures of LAO {101} and anatase {101} of the thin film prepared by TTIP-nPr and annealed at 800°C

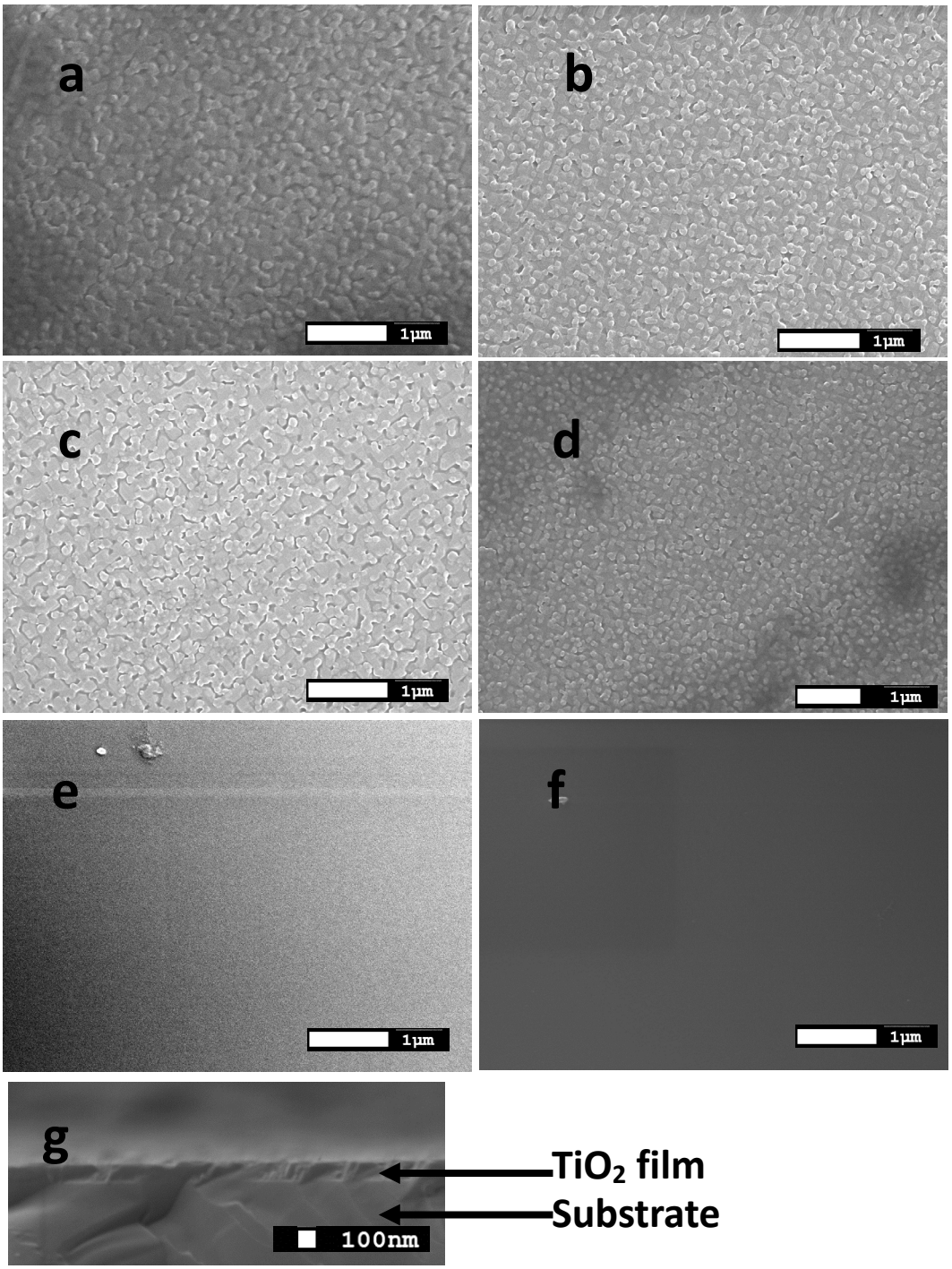

Figure 7. SEM images of each thin of each thin film and annealed at 800°C (a) TTIP-nPr, (b) TTIP-nBu, (c) TTBu-nPr, (d) TTBu-nBu (e) 250°C annealed thin film prepared by TTIP-nBu solvent mixture and (f) $LaALO_3$ substrate (g) Cross sectional view of thin film made by TTIP=nPr solvent mixture ** at 15 kV tension and 8 mA probe current**

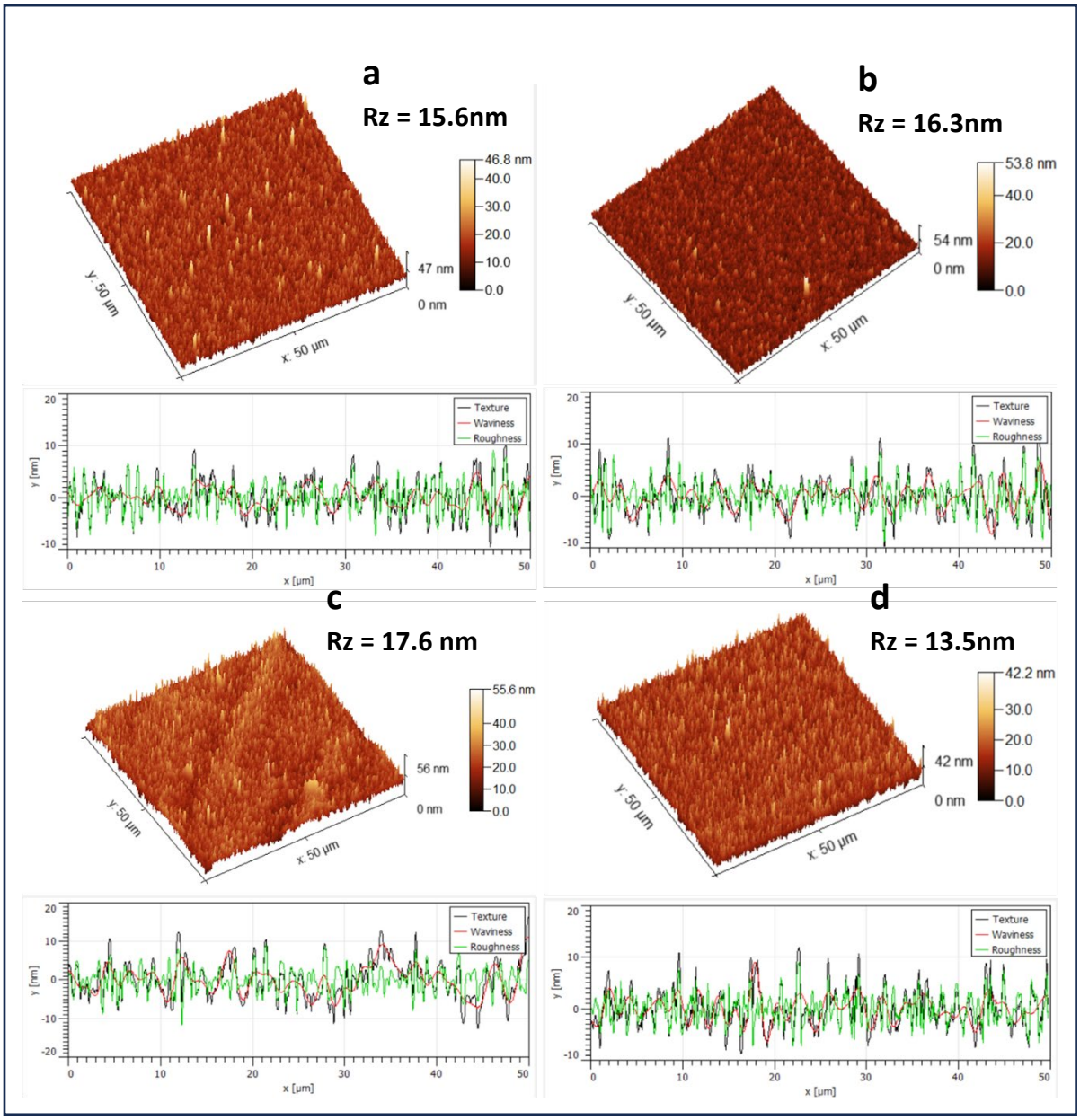

Figure 8. AFM 3D images of each thin of each thin film and annealed at 800°C (a) TTIP-nPr, (b) TTIP-nBu, (c) TTBu-nPr, (d) TTBu-nBu

Supplementary materials

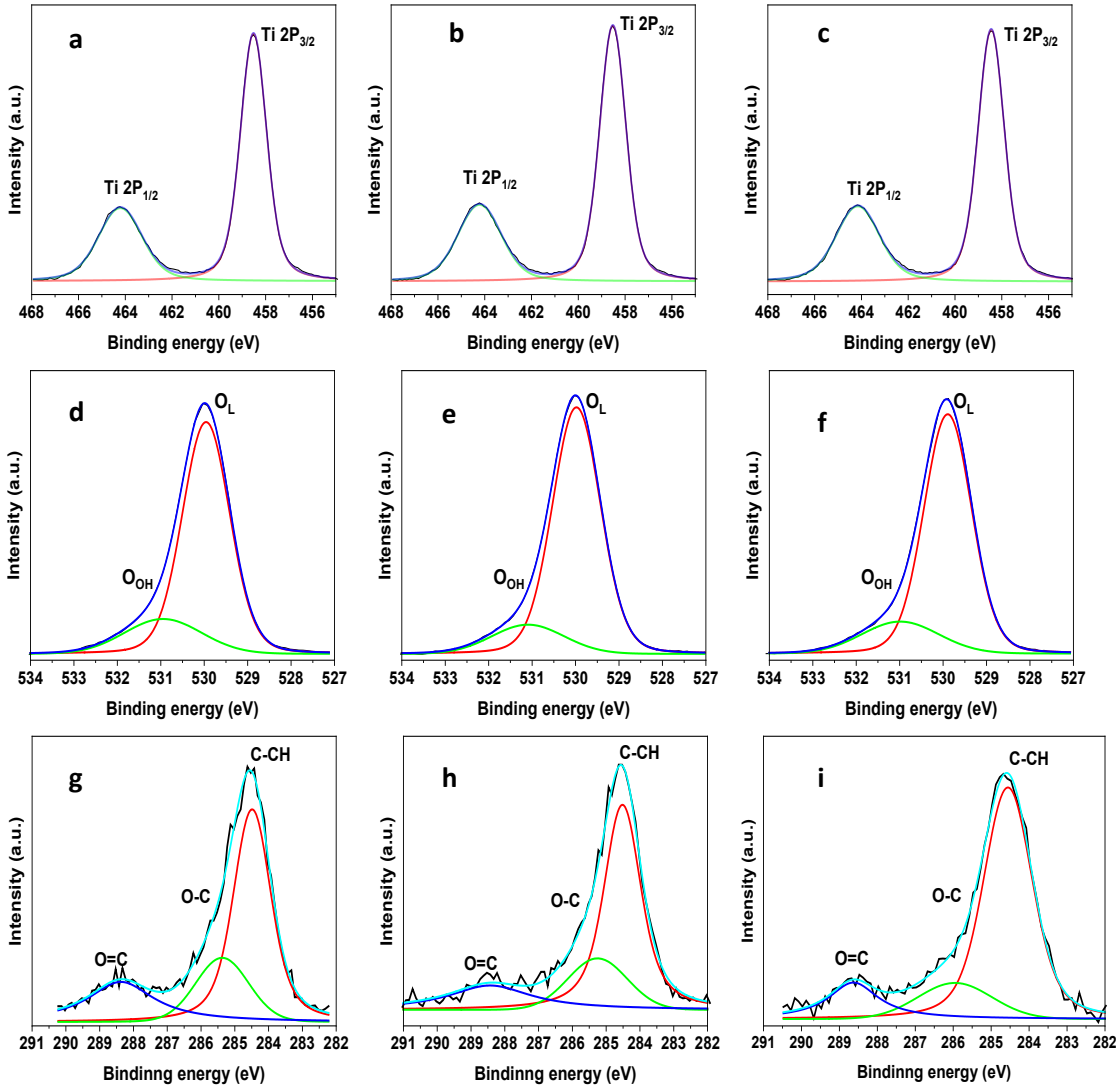

Figure S1. deconvoluted high resolution XPS spectra of Ti 2p and O 1s regions thin films annealed at 800 °C. (a) Ti 2p region of TTIP-nPr film (b) Ti 2p region of TTBu-nPr film, (c) Ti 2p region of TTBu-nBu, (d) O1s region of TTIP-nPr film, (e) O1s region of TTBu-nPr film, (f) O1s region of TTBu-nBu film (g) C1s region of TTIP-nPr film (h) C1s region of TTBu-nPr film and (i) C1s region of TTBu-nBu film.

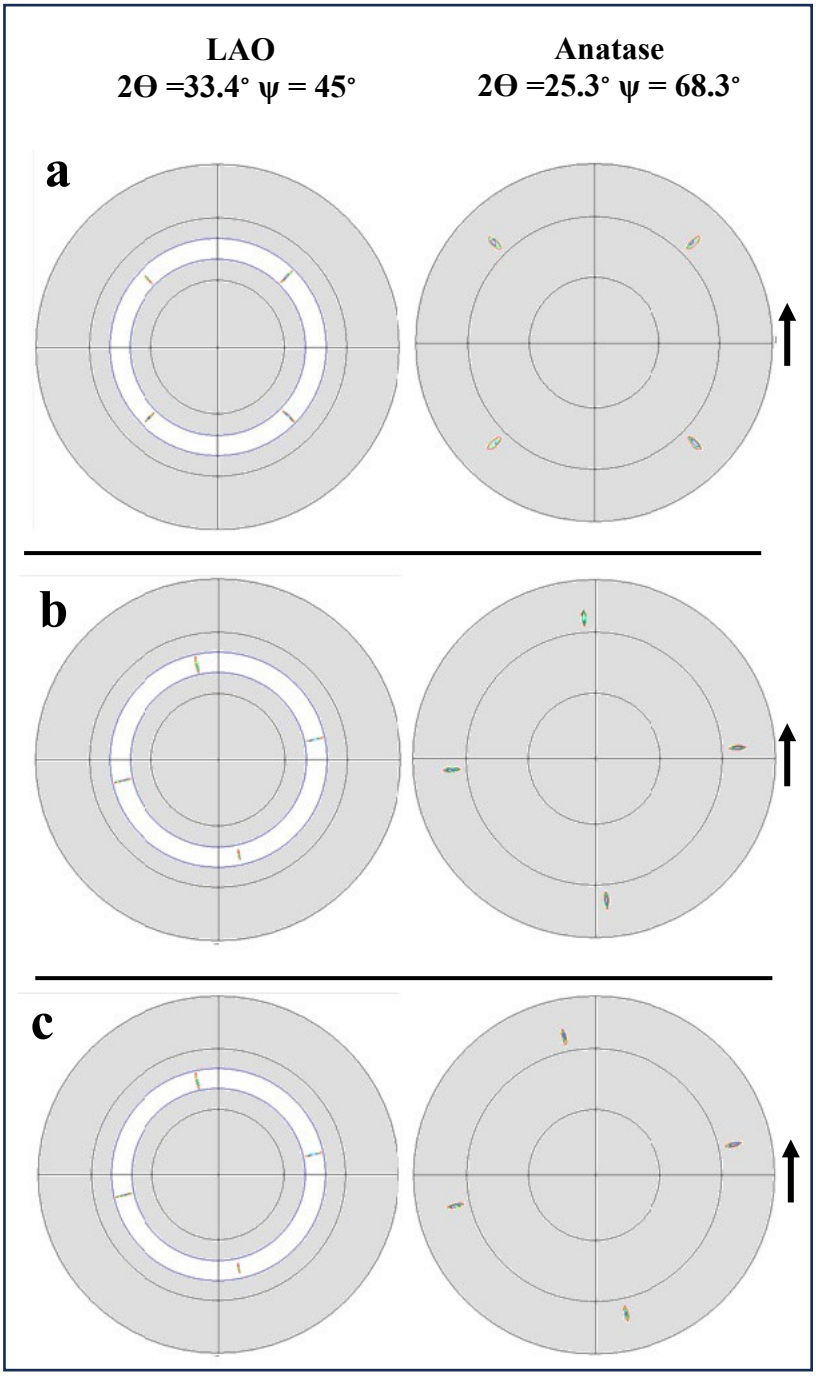

Figure S2. Orientation analysis by pole figures of LAO {101} and anatase {101} of the thin film prepared at annealed at 800°C (a) TTIP-nBu film (b) TTBu-nPr film, and (c) TTBu-nBu film.

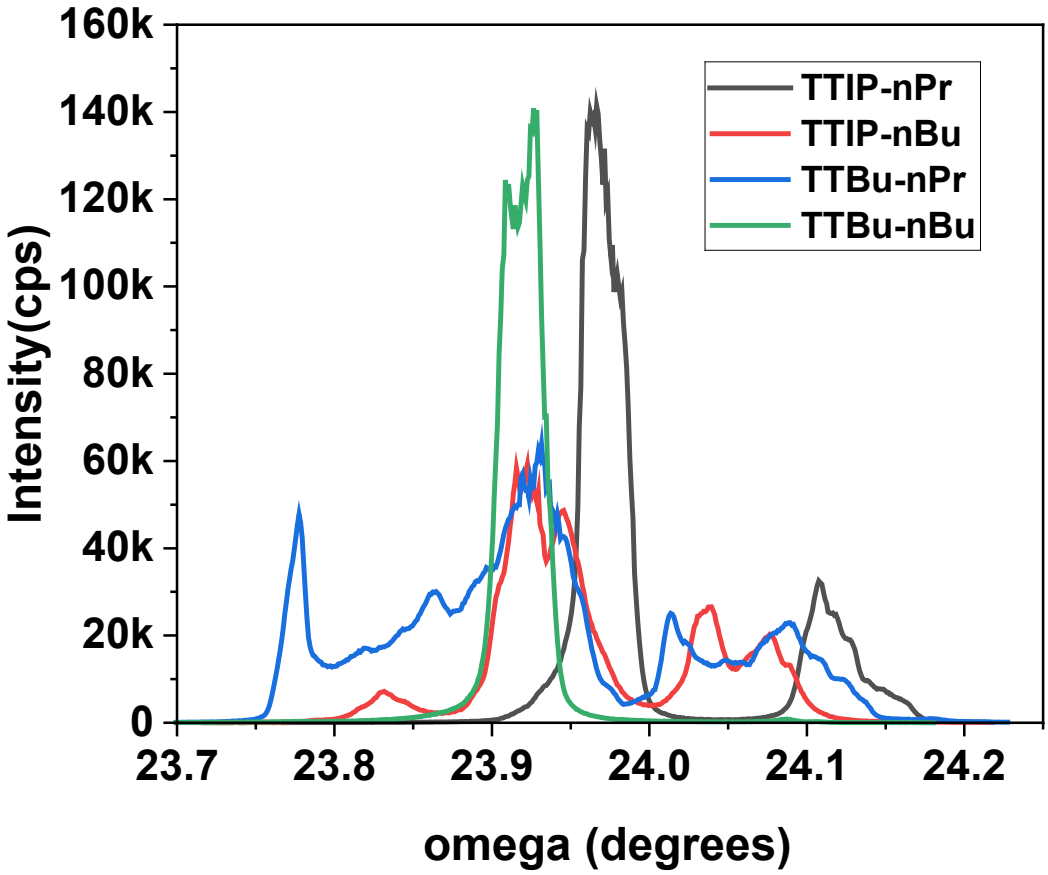

Figure S3. XRD rocking curves of each $LaAlO_3$ substrates 800 °C